Implications of the Steady-state Assumption for the Global Vegetation Carbon Turnover

Naixin Fan[1,2*], Maurizio Santoro[3], Simon Besnard[4], Oliver Cartus[3], Sujan Koirala[1] and Nuno Carvalhais[1,5*]

[1]Max Planck Institute for Biogeochemistry, Hans Knöll Strasse 10, 07745 Jena, Germany

[2]Technische Universität Dresden, Institute of Photogrammetry and Remote Sensing, Helmholtzstr. 10, 01069, Dresden, Germany

[3]Gamma Remote Sensing, 3073 Gümligen, Switzerland

[4]Laboratory of Geo-Information Science and Remote Sensing, Wageningen University & Research, The Netherlands

[5]Departamento de Ciências e Engenharia do Ambiente, DCEA, Faculdade de Ciências e Tecnologia, FCT, Universidade Nova de Lisboa, 2829-516 Caparica, Portugal

* Corresponding authors: Naixin Fan (nfan@bgc-jena.mpg.de) and Nuno Carvalhais (ncarvalhais@bgc-jena.mpg.de)

Key Points:

- We estimate vegetation carbon turnover times globally in a non-steady state from 1992 to 2016.

- Using the assumption of steady-state for vegetation biomass turnover can cause substantial biases locally.

- The validity of steady-state assumption increases with spatial scales.

24 **Abstract**

25 Vegetation turnover time (τ) is a central ecosystem property to quantify the global vegetation
26 carbon dynamics. However, our understanding of vegetation dynamics is hampered by the lack
27 of long-term observations of the changes in vegetation biomass. Here we challenge the steady
28 state assumption of τ by using annual changes in vegetation biomass that derived from remote-
29 sensing observations. We evaluate the changes in magnitude, spatial patterns, and uncertainties
30 in vegetation carbon turnover times from 1992 to 2016. We found that the forest ecosystem is
31 close to a steady state at global scale, contrasting with the larger differences between τ under
32 steady state and τ under non-steady state at the grid cell level. The observation that terrestrial
33 ecosystems are not in a steady state locally is deemed crucial when studying vegetation dynamics
34 and the potential response of biomass to disturbance and climatic changes.

35 **Plain Language Summary**

36 Previous studies relied on the assumption that vegetation carbon turnover does not change with
37 time. However, this assumption can be substantially violated under the influence of disturbances
38 such as climate change and land use. We compared the difference of carbon turnover estimations
39 under different assumptions by using a global observations of vegetation biomass.

40

41 **1 Introduction**

42   One of the largest uncertainties in Earth system models is in quantifying how the carbon
43 uptake by terrestrial ecosystems will respond to changes in climate (Friedlingstein et al. 2006;
44 Friend et al., 2014). As an emergent ecosystem property that partially determines carbon
45 sequestration capacity, the vegetation biomass turnover times (τ) have been used as a diagnostic
46 metric to quantify the feedback between the carbon cycle and climate (Carvalhais et al., 2014;
47 Thurner et al., 2016). However, there is a large uncertainty in the simulations of vegetation
48 carbon stock as well as τ across earth system models, indicating different representations of the
49 response of vegetation to future climate change (Friend et al. 2014). Furthermore, our current
50 understanding of τ and the dynamic of vegetation is limited due to the lack of long-term
51 observations of changes in vegetation. As a result, the estimation of τ has relied so far on the
52 assumption that the vegetation carbon in an ecosystem will eventually reach a steady state
53 (steady state assumption, hereafter SSA) at which the net change of vegetation biomass becomes
54 zero (ΔC_{veg}=0), or so small compared to the total biomass that becomes negligible. The SSA has
55 been shown to be a useful assumption at a large spatial scale. However, at local scales, an
56 ecosystem is unlikely to maintain a steady state due to the influences from external factors such
57 as disturbances and climate variability (Ge et al., 2019). It is still unknown whether the SSA can
58 hold at local spatial domains and how much the difference it can make to the τ estimation if one
59 neglects the temporal changes in vegetation carbon.

60   In this study, we used estimates of annual changes in vegetation carbon derived from a
61 multi-decadal dataset and global estimations of gross primary productivity (GPP) that are driven
62 by meteorological observations (Besnard et al., 2021; Santoro et al., 2022; Tramontana et al.
63 2016; Jung et al. 2020), for estimating and comparing τ estimates that are derived from SSA and
64 non-steady-state assumption (hereafter NSSA), respectively, at local, biome and global scales.
65 The validity of SSA was evaluated in different spatial domains to better quantify the effect of
66 spatial scales on the patterns of carbon turnover times.

2 Data and Methods

In this section, we first introduce the datasets we used to estimate τ including above-ground vegetation biomass, below-ground biomass and gross primary productivity. We used a forest canopy cover dataset to examine the relationship between the changes in τ and tree canopy cover. Then the calculations of τ using three methods are introduced next with detailed explanations.

2.1 The multi-decadal estimates of AGB dataset

Annual AGB estimates were derived from C-band satellite radar signals between 1992 and 2016 with a pixel size of 25 km (Santoro et al., 2022). The very dense time series of observations by the European Remote Sensing (ERS) WindScatterometer, the MetOp Advanced SCATterometer (ASCAT), and the Envisat Advanced Synthetic Aperture Radar (ASAR) were used to maximize the information content of forest structure in the signal, allowing for AGB estimates of higher accuracy compared to values obtained from a single observation (Santoro et al., 2022). The annual estimation of AGB is obtained by synthesizing all daily observations of the radar backscatter at one location in a pixel (0.25°×0.25°), enabling the inference of a continuous time series of AGB estimation. By adapting the AGB retrieval method in time and space and computing a weighted average of individual AGB estimates, the annual AGB estimates were less impacted by data noise, instantaneous moisture conditions, precipitation, and snow cover (Santoro et al., 2011).

2.2 Estimation of total vegetation carbon stock

The stock of total vegetation biomass consists of AGB and BGB. Therefore, we estimated BGB from the AGB time series by scaling with the root-shoot ratio, Rrs:

$$BGB = AGB \times R_{rs} \ (1)$$

In this study, we used a spatially explicit global dataset of root-shoot ratio, which was derived from a machine learning model that is trained on a large number of ground field measurements of forest root biomass as a function of shoot biomass, tree height, age, species, topography, land management, edaphic and climate covariates (Huang et al., 2021).

The total vegetation carbon was obtained by summing the carbon in both AGB and BGB under the assumption that the carbon stock is 47% of the total dry biomass (IPCC, 2006):

$$C_{veg} = AGB \times (1 + R_{rs}) * 0.47 \ (2)$$

2.3 GPP dataset

We used estimations of GPP from the FLUXCOM project in which different machine learning approaches were applied to upscale global energy and carbon fluxes from eddy covariance flux measurements (Tramontana et al., 2016; Jung et al., 2020). In this study, GPP annual estimates driven by meteorological observations and remote sensing

104 observations at the spatial resolution of 0.5º and the time period from 1992 to 2016 are
105 used as carbon influx into the vegetation carbon pool. The dataset was resampled to the
106 spatial resolution of 0.25º to match the AGB dataset.

107

108 2.4 Forest tree canopy cover change

109 Tree canopy cover (vegetation that is greater than 5 meters in height) was derived from
110 the Advanced Very High Resolution Radiometer (AVHRR) remote-sensing
111 measurements (Song et al., 2018). The version 4 Long Term Data Record (LTDR) was
112 used to generate the data on tree canopy coverage from 1982 to 2016. Daily LTDR
113 surface reflectance data were used to compute the normalized difference vegetation index
114 (NDVI) at each pixel (0.05º×0.05º). Maximum NDVI composition was then used to
115 obtain adjusted annual phenological metrics, which were used as input to supervised
116 regression tree models to generate the annual product of tree canopy coverage.

117

118 2.5 Estimation of τ under steady state

119 Changing C_{veg} over time is determined by the uptake of carbon and turnover times:

120
$$\frac{dC_{veg}}{dt} = GPP - \frac{C_{veg}}{\tau} \quad (3)$$

121 C_{veg} is the vegetation carbon stock. Assuming that the vegetation carbon pool is in a
122 steady state, i.e., the change in C_{veg} over time (dC_{veg}/dt) equals zero, then vegetation
123 carbon turnover times can be calculated as the ratio between vegetation carbon stock and
124 GPP:

125
$$\tau_{SSA} = \frac{C_{veg}}{GPP} \quad (4)$$

126 Here τSSA is calculated pixel-wise by using annual mean C_{veg} and GPP over the period
127 of 1992-2016.

128

129 2.6 Estimation of τ under non-steady state

130 Compared with the estimations of τ under steady-state assumption, the changes in C_{veg}
131 over time are considered ($dC_{veg}/dt \neq 0$) when estimating τ under non-steady state (τ_{NSSA}).

132   To derive a robust estimation of τ_{NSSA} at each grid cell, we calculated τ_{NSSA} using three
133   different methods to assess the uncertainty built in the τ estimations.

134   Method 1

135   We estimate ΔC_{veg} by calculating the annual difference of C_{veg} between year t and year t
136   − 1. Then, a τ estimate can be derived for each year by applying GPP and ΔC_{veg} at year t.
137   Finally, we derive the τ under a non-steady state by averaging over time:

138
$$\tau_{NSSA} = \frac{C_{veg,t-1}}{GPP_t - \Delta C_{veg,t}} \quad (5)$$

139   Method 2

140   In the second method, we estimated the mean ΔC_{veg} using the trend of C_{veg} in a certain
141   period to avoid the influence of outliers on the results. In this way, τ can be inferred as:

142
$$\tau_{NSSA} = \frac{\overline{C_{veg}}}{\overline{GPP} - \Delta C_{veg,trend}} \quad (6)$$

143   Here the $\Delta C_{veg,trend}$ is inferred by applying a simple linear regression model (least-
144   square robust fitting) between the response variable C_{veg} and time ($C_{veg} \sim T$). The
145   coefficient of T is, therefore, the average annual ΔC_{veg} over the whole period. Thus, the τ
146   under a non-steady state can be estimated with the annual mean values of C_{veg}, GPP, and
147   ΔC_{veg}.

148

149   Method 3

150   In the third method, we infer τ from Eq.3 by applying a linear regression model (least-
151   square robust fitting) at each grid cell in which (GPP - ΔC_{veg}) is the target variable while

152   C_{veg} is the predictor, enabling annual turnover time to be inferred from the coefficient of

153   C_{veg} (1/ τ_{NSSA}):

154

$$GPP - \Delta C_{veg} \sim \frac{1}{\tau_{NSSA}} \cdot C_{veg} \quad (7)$$

155   Here ΔC_{veg} is the difference of C_{veg} between year t and year t - 1. GPP is the carbon input

156   in year t and C_{veg} is the total carbon density in year t - 1, respectively.

157

3 Results

159   3.1 Comparison of τ under NSSA and SSA at grid cell level and global scale

160   The τ values (Figure 1) represent the turnover time of the entire forest living vegetation

161   biomass, averaged over the whole period of the observations. The comparison between

162   estimates of τ_{NSSA} using three different methods and τ_{SSA} shows a consistent pattern that

163   carbon turnover processes are far from a steady state at the grid cell level (Figure S1).

164   Although there is a high correlation in the global spatial patterns (R2>0.98, bottom off-

165   diagonal plots in Figure 1), differences between τ_{NSSA} and τ_{SSA} are characterized by high

166   spatial heterogeneity. Although there are differences in the estimations of τ_{NSSA} that derived

167   from the three methods, the high global correlation and similar patterns of the difference

168   between τ_{NSSA} and τ_{SSA} shows high consistency in the estimated τ_{NSSA}. Our results show a

169   high spatial variability of τ values ranging from 0 to 15 years. The longest turnover times

170   are located in the northern boreal forest ecosystem, where part of the biome has τ values

171   longer than ten years, whereas carbon in the temperate forest ecosystem turnovers over

172   much faster where the τ values are mostly under five years. The assumption that vegetation

173   biomass is in steady state results in an overall bias of τ by 10% (90th percentile), compared

174   to the τ estimates under a non-steady state at the grid cell level (Figure 1). This finding

175   indicates that the majority of global forest ecosystems are not in a steady state, although

176   the degree of deviation from a steady state differs from one region to another. The

177   discrepancies between τ_{SSA} and τ_{NSSA} are substantially higher in the boreal forest (4.33%)

178   ecosystem than in the tropical forest 10.99%) ecosystems indicating that the forests in the

179   tropics are closer to a steady state, whereas assuming SSA in the boreal forest may cause

180   large bias (Figure S2). Although the difference can be large at the grid cell level, there is a

181   high global correlation (r > 0.98) between τ_{SSA} and τ_{NSSA} at the global scale, indicating an

182   overall similar spatial pattern with or without considering the changes in annual biomass

183   at the global scale. Here we show that the forest biomass at the global scale is roughly in a

184   steady state whereas the SSA is largely violated at the grid cell level, especially in the

185   northern boreal forest ecosystems where the τ values can be substantially underestimated

186   or overestimated if assuming SSA.

187   In line with a previous study in which the SSA-induced biases are assessed at site level (Ge

188   et al., 2019), we show that SSA causes significant underestimations of τ up to 40% (99th

189   percentile) in China during the period of 2005-2015 (Figure S3). However, our results show

190   a high heterogeneity where SSA can also cause overestimation of τ up to -12% (1th

191 percentile). Further analysis shows that the pattern also changes across different periods of
192 time. For instance, there is a contrasting pattern between 2001-2005 and 2009-2013 in
193 which the former is characterized by overestimation of τ induced by SSA whereas there is
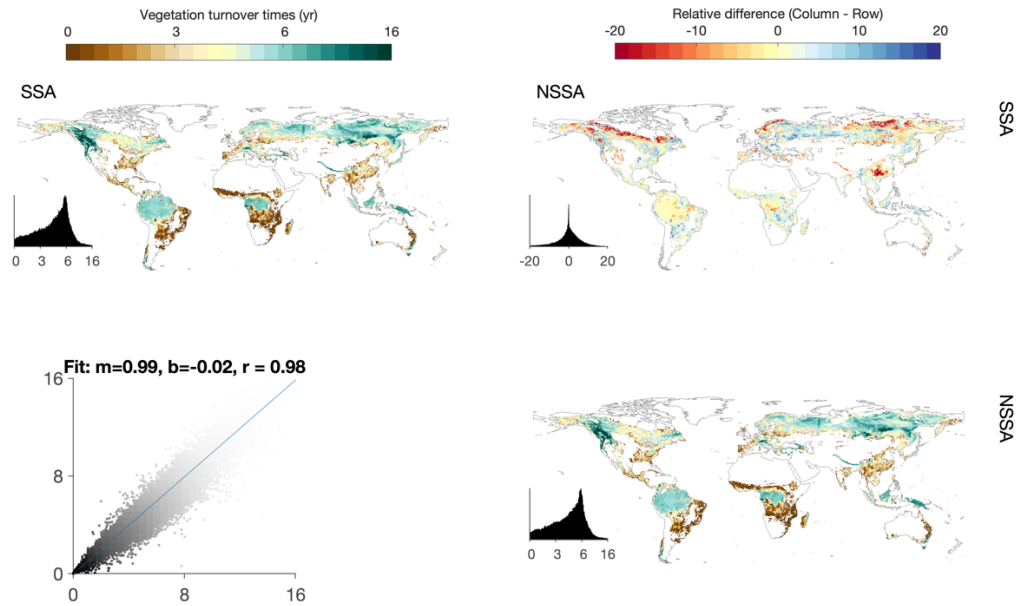194 a widespread underestimation of τ in the latter.

195

196

197 **Figure 1**. Comparison of τ under SSA and NSSA. The upper off-diagonal subplots show
198 the relative difference between each pair of datasets (column/row). The bottom off-
199 diagonal subplots show the density plots and major axis regression line between each pair
200 of datasets (m: slope, b: intercept, r: correlation coefficient). The ranges of both of the
201 color bars are between the 1st and the 99th percentiles of the data.

202

203 3.2 The effect of large-scale disturbances on carbon turnover times

204 The disturbance from natural causes or anthropogenic activities can make an ecosystem
205 deviate from a steady state. By estimating carbon turnover times at different periods, we
206 quantified the degree of deviation if disturbances, e.g., deforestation, happened in a forest
207 ecosystem. Figure 2 shows that the pervasive deforestation in the 90s primarily affected
208 the carbon turnover times in the southeast part of the Amazon, which is known as the 'arc
209 of deforestation' (hereafter AOD, Durieux et al., 2003). Our results clearly show τ_{NSSA} is
210 approximately 20% lower than τ_{SSA} in the AOD region from 1993 to 1998, indicating

anthropogenic activity (mostly deforestation) accelerated the carbon turnover rates to a large extent. Compared with the AOD, forests in the middle of Amazon, where there are less population and disturbances, are closer to a steady state, as shown by the much less difference between τ_{NSSA} and τ_{SSA}. Further analysis shows that tree canopy cover (Figure 2, Row 2) and C_{veg} (Figure 2, Row 3) changes decreased mainly during the same period of 1993-1998, whereas the changes in GPP does not follow the trend in the arc of deforestation. These results indicate that the acceleration of turnover times during this period is directly caused by the large decrease in the vegetation biomass, which is intimately associated with a decrease in forest cover in this region. On the other hand, our findings show that the forest ecosystems started to recover during the 1999-2004 period as the vegetation biomass increased by 10% to 20%, in line with the increased tree canopy cover in the AOD region. As a result, the carbon turnover times increased by 10% to 30% during the same period. From 2011 to 2016, the magnitude of changes in τ, C_{veg} and tree canopy cover significantly decreased, indicating the forest ecosystems are closer to a steady state due to less disturbances. These findings indicate that turnover times and the steady state of the forest ecosystem can be largely affected by anthropogenic activities.
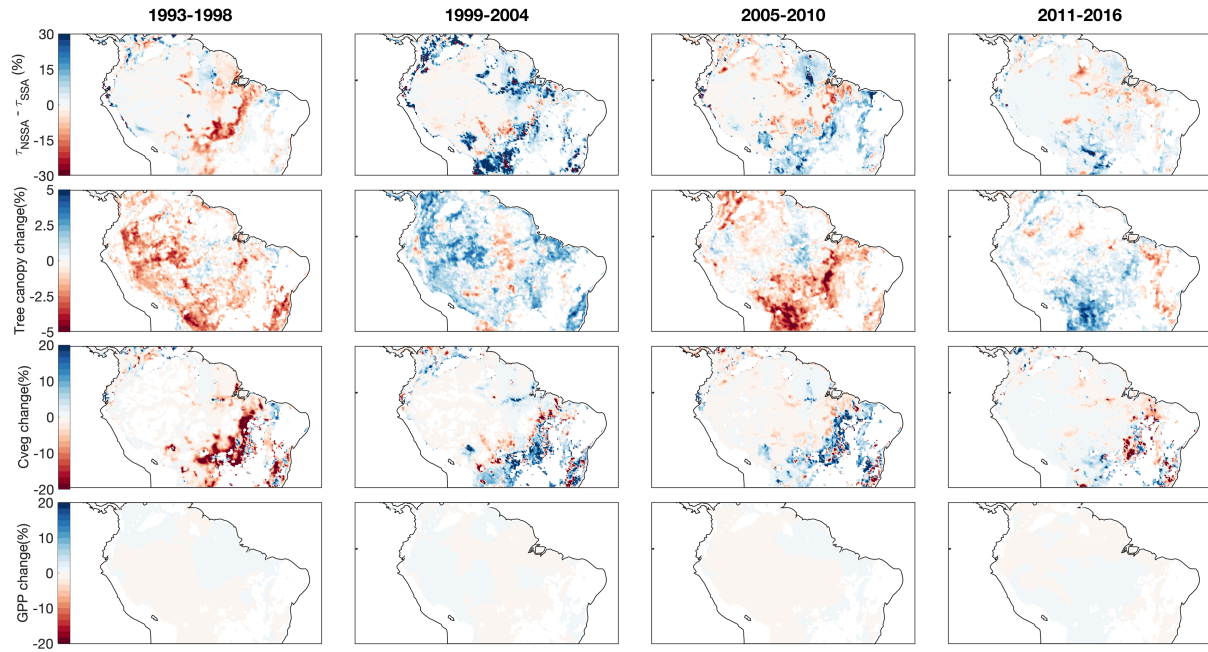

Figure 2. Regional changes in the relative difference between τ_{NSSA} and τ_{SSA} ((τ_{NSSA} - τ_{SSA})/ τ_{SSA}*100) from 1993 to 2016, row 1, forest cover change (%), row 2, vegetation

232 biomass change (%), row 3, GPP change (%), row 4 at different time periods in Amazon
233 region.

234

235 3.3 The effect of spatial scale on the steady-state assumption

236 We further investigate the effect of spatial scale on the difference between τ_{NSSA} and τ_{SSA}
237 in different biomes by gradually changing the spatial scale from 0.25º (grid cell level) to
238 25º (continental scale) as shown in Figure 3. Here the difference between τ_{NSSA} and τ_{SSA} at
239 each spatial scale is quantified by the 10, 50 and 90 percentiles of the relative difference
240 between τ_{NSSA} and τ_{SSA} (Q_{10}, Q_{50}, Q_{90}, Figure 4). We find that the difference between τ_{NSSA}
241 and τ_{SSA} substantially decreases with increasing spatial scales. The Q_{10} and Q_{90} tropical
242 forests decrease by approximately 5%, whereas it decreases by approximately 10% in
243 temperate and boreal biomes when the spatial scale increases from grid cell to ecosystem
244 scale. Globally, the difference between τ_{NSSA} and τ_{SSA} is approximately 3% at ecosystem
245 scale, indicating that steady state assumption will cause less errors in estimating carbon
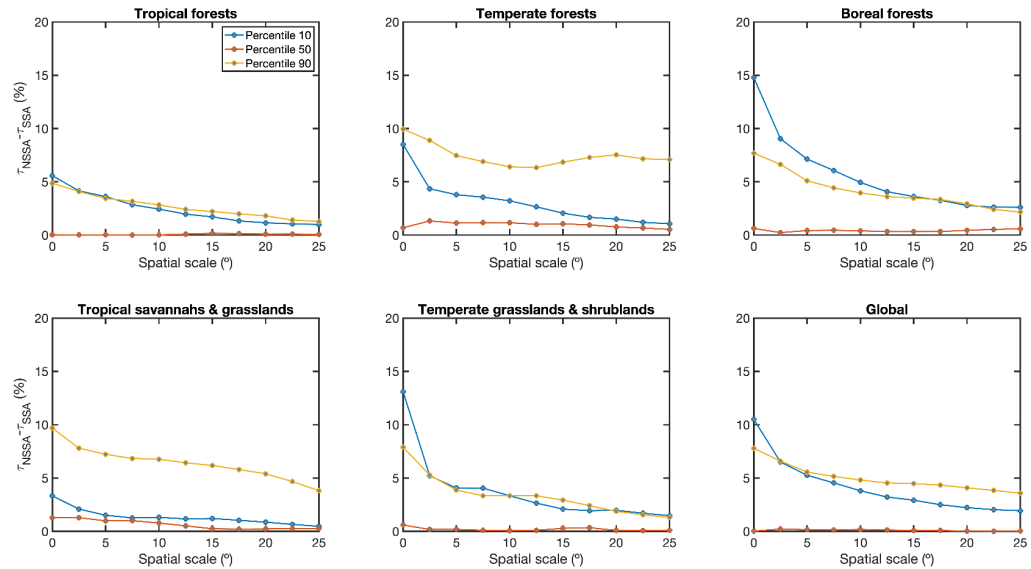246 turnover times at larger spatial scales.

247

248 **Figure 3**. Effects of spatial scale on the difference between τ_{SSA} and τ_{NSSA}. The x-axis
249 represents the increase of spatial scales from grid cell level (0.25º) to continental level
250 (25º). The y-axis represents the 10th (absolute value) and 90th relative difference between
251 τ_{NSSA} and τ_{SSA}.

252

4 Discussion

254 Our findings imply that the two different assumptions, i.e., SSA and NSSA, should be
255 applied based on different ecological principles and spatial scales. The common approach

of defining τ as the ratio between carbon stock and carbon influx based on SSA can be justified and properly applied when the changes in net carbon flux are negligible relative to the total carbon stock (Carvalhais et al., 2014). Although disturbances from nature or human beings could cause non-steady-state behavior, neglecting the changes, in some cases, only make a little difference to the quantification of the spatial pattern of τ, which does not hamper the understanding of the dynamics of the terrestrial ecosystem carbon cycle. However, at a grid cell level, neglecting the changes in vegetation carbon (assuming vegetation is in a steady state) may result in a large bias. Using three methods, we provide robust estimations of τ under a non-steady state. The comparisons between τ_{SSA} and τ_{NSSA} show high heterogeneity in both space and time. A pioneer study (Ge et al., 2019) showed large SSA-induced biases on τ estimation in varied ecosystems of China by using the data at ten FLUXNET sites from 2005 to 2015 which is consistent with our results. However, we further show that the magnitude and the signs of the SSA-induced biases are characterized by high spatial heterogeneity and can change in time. This is mainly caused by the changes in vegetation biomass due to climate change or disturbances (Figure 2).

We have shown substantial heterogeneity in the degree of validity of the steady-state assumption across space. The comparison between τ_{SSA} and τ_{NSSA} quantitatively shows that most global forest ecosystems are far from steady-state, especially in the temperate and boreal forests. Even at regions of high biomass density such as Amazon Forest where the changes in vegetation carbon is relatively small, i.e., closer to steady-state, disturbances such as deforestation or fire could drive the forest ecosystem away from steady-state, as our results clearly show that the arc of deforestation in Amazon Forest have large difference between τ_{SSA} and τ_{NSSA} caused by drastic changes in vegetation biomass (Figure 2). These results indicate that applying SSA at the grid cell level is likely to cause substantial errors, potentially leading to misleading conclusions based on poor estimation of carbon turnover times.

Furthermore, our study quantified the link between spatial scales and the validity of SSA. Our results imply that SSA is approximately valid at large spatial scales (>15º or 1500km), at which scale the differences are much lower (~5%) than grid cell level. The current understanding of the temporal dynamics of the terrestrial carbon cycle nearly all relies on earth system models in which the carbon turnover rates are retrieved under the SSA, which results in large discrepancies in carbon pools and turnover among different models (Friend et al., 2014; Todd-Brown et al., 2013). The estimation of τ under NSSA with observational long-term biomass data provides insights into better understanding and thus modeling turnover rate and its spatial patterns.

5 Implications, Limitations and Conclusions

Although we used different streams of data and methods to account for the uncertainties in the estimations of carbon turnover, several factors may limit the results of our study. First, the estimations of AGB by Santoro et al. (2022) is derived at relatively coarse spatial resolution at 0.25º which makes it impossible to compare with measurements of AGB at plot level. To overcome the limitation, Santoro et al. relied on gridded datasets including a

vegetation density map, an independent AGB map, a global land cover map and a model of global elevation to estimate the unknown model parameters that are necessary to infer vegetation biomass. Second, the estimated total vegetation carbon stock is calculated by using a spatial explicit root-shoot ratio of biomass that does not change with time. Therefore, we assume that the relationship between above- and below-ground biomass does not have a directional change over long-term in this study. Nevertheless, our findings suggest that the steady state assumption is robust at a global scale yet becomes much less realistic at the grid cell level as the difference between regional τ_{SSA} and τ_{NSSA} can be as large as 20%. The usage of the steady state assumption would result in a substantial bias of τ, especially in the northern boreal forest ecosystems and regions with a high degree of disturbance, either from anthropogenic sources or natural factors. However, at a larger spatial scale, the differences in τ estimations at SSA and NSSA significantly decrease because the annual changes in vegetation biomass are small compared with the total amount of biomass. With the novel long-term observations of vegetation biomass, we revealed a detailed picture of the spatial distribution of carbon turnover times under different assumptions and its relationship with spatial scales, which will guide the proper application of the two assumptions on different conditions.

Acknowledgments

Author Contributions

N.F. and N.C. designed the analysis of this research and wrote the manuscript with contributions from all authors.

Data availability

The estimates of vegetation carbon turnover times that supports the findings of this research are temporarilty available in https://figshare.com/s/c542bf749f76c8937eaa. Please note that the data will be permanently available in figshare.com upon the acceptance of this paper.

329

330

References

Besnard, S., Santoro, M., Cartus, O., Fan, N., Linscheid, N., Nair, R., et al. (2021). Global
sensitivities of forest carbon changes to environmental conditions. *Global Change
Biology*, *27*(24), 6467–6483. https://doi.org/10.1111/gcb.15877

Carvalhais, N., Forkel, M., Khomik, M., Bellarby, J., Jung, M., Migliavacca, M., et al. (2014).
Global covariation of carbon turnover times with climate in terrestrial ecosystems.
Nature, *514*(7521), 213–217. https://doi.org/10.1038/nature13731

Durieux, L., Machado, L. A. T., & Laurent, H. (2003). The impact of deforestation on cloud
cover over the Amazon arc of deforestation. *Remote Sensing of Environment*, *86*(1), 132–
140. https://doi.org/10.1016/S0034-4257(03)00095-6

Eggleston, H. S., Buendia, L., Miwa, K., Ngara, T., & Tanabe, K. (2006a). 2006 IPCC
Guidelines for National Greenhouse Gas Inventories. Retrieved from
https://www.osti.gov/etdeweb/biblio/20880391

Eggleston, H. S., Buendia, L., Miwa, K., Ngara, T., & Tanabe, K. (2006b). 2006 IPCC
guidelines for national greenhouse gas inventories.

Friedlingstein, P., Cox, P., Betts, R., Bopp, L., Bloh, W. von, Brovkin, V., et al. (2006). Climate–
Carbon Cycle Feedback Analysis: Results from the C4MIP Model Intercomparison.
Journal of Climate, *19*(14), 3337–3353. https://doi.org/10.1175/JCLI3800.1

Friend, A. D., Lucht, W., Rademacher, T. T., Keribin, R., Betts, R., Cadule, P., et al. (2014).
Carbon residence time dominates uncertainty in terrestrial vegetation responses to future

351   climate and atmospheric CO2. *Proceedings of the National Academy of Sciences*, *111*(9),

352   3280–3285. https://doi.org/10.1073/pnas.1222477110

353   Ge, R., He, H., Ren, X., Zhang, L., Yu, G., Smallman, T. L., et al. (2019). Underestimated

354   ecosystem carbon turnover time and sequestration under the steady state assumption: A

355   perspective from long-term data assimilation. *Global Change Biology*, *25*(3), 938–953.

356   https://doi.org/10.1111/gcb.14547

357   Huang, Y., Ciais, P., Santoro, M., Makowski, D., Chave, J., Schepaschenko, D., et al. (2021). A

358   global map of root biomass across the world's forests. *Earth System Science Data*, *13*(9),

359   4263–4274. https://doi.org/10.5194/essd-13-4263-2021

360   Jung, M., Schwalm, C., Migliavacca, M., Walther, S., Camps-Valls, G., Koirala, S., et al. (2020).

361   Scaling carbon fluxes from eddy covariance sites to globe: synthesis and evaluation of

362   the FLUXCOM approach. *Biogeosciences*, *17*(5), 1343–1365. https://doi.org/10.5194/bg-

363   17-1343-2020

364   Santoro, M., Beer, C., Cartus, O., Schmullius, C., Shvidenko, A., McCallum, I., et al. (2011).

365   Retrieval of growing stock volume in boreal forest using hyper-temporal series of Envisat

366   ASAR ScanSAR backscatter measurements. *Remote Sensing of Environment*, *115*(2),

367   490–507.

368   Santoro, M., Cartus, O., Wegmüller, U., Besnard, S., Carvalhais, N., Araza, A., et al. (2022).

369   Global estimation of above-ground biomass from spaceborne C-band scatterometer

370   observations aided by LiDAR metrics of vegetation structure. *Remote Sensing of*

371   *Environment*, *279*, 113114. https://doi.org/10.1016/j.rse.2022.113114

372 Song, X.-P., Hansen, M. C., Stehman, S. V., Potapov, P. V., Tyukavina, A., Vermote, E. F., &

373   Townshend, J. R. (2018). Global land change from 1982 to 2016. *Nature*, *560*(7720),

374   639–643. https://doi.org/10.1038/s41586-018-0411-9

375 Thurner, M., Beer, C., Carvalhais, N., Forkel, M., Santoro, M., Tum, M., & Schmullius, C.

376   (2016). Large-scale variation in boreal and temperate forest carbon turnover rate related

377   to climate. *Geophysical Research Letters*, *43*(9), 4576–4585.

378   https://doi.org/10.1002/2016GL068794

379 Todd-Brown, K. E., Randerson, J. T., Post, W. M., Hoffman, F. M., Tarnocai, C., Schuur, E. A.,

380   & Allison, S. D. (2013). Causes of variation in soil carbon simulations from CMIP5 Earth

381   system models and comparison with observations. *Biogeosciences*, *10*(3).

382 Tramontana, G., Jung, M., Schwalm, C. R., Ichii, K., Camps-Valls, G., Ráduly, B., et al. (2016).

383   Predicting carbon dioxide and energy fluxes across global FLUXNET sites with

384   regression algorithms. *Biogeosciences*, *13*(14), 4291–4313. https://doi.org/10.5194/bg-

385   13-4291-2016

386

387

388